# Thermoelectric Performance Model Development and Validation for a Selection and Design Tool

Thomas Nunnally, Devin Pellicone, Nathan Van Velson, James Schmidt, Tapan Desai
Advanced Cooling Technologies, Inc.
1046 New Holland Ave.
Lancaster, PA, USA 17601

Email: thomas.nunnally@1-act.com

## ABSTRACT

A thermal model has been developed to simulate the performance of thermoelectric cooling for two avionics scenarios, where utilizing commercial off the shelf (COTS) components is highly desirable. Modeling predictions were validated through a series of experiments which studied the two scenarios at varying heat loads and heat sink thermal resistances. In these experiments, component temperatures were shown to be reduced by up to 15% with the addition of a thermoelectric cooler. Furthermore, in both scenarios, the model predicted the temperature of the cooled components within 3-10% accuracy. Further development of the model could result in a tool, which is not currently available, for optimizing system performance and determining the applicability of thermoelectric cooling in a given scenario.

**KEY WORDS:** thermoelectric cooling, COTS, thermal modeling, avionics, thermal management

## NOMENCLATURE

| | |
|---|---|
| TEC | thermoelectric cooler |
| $Z$ | thermoelectric figure of merit, $K^{-1}$ |
| $Q_c$ | heat absorbed at cold surface, W |
| $Q_h$ | heat rejected, W |
| $P_{TEC}$ | TEC power consumption, W |
| $T_h$ | hot side temperature, K |
| $T_c$ | cold side temperature, K |
| $\Delta T$ | $T_h$ - $T_c$, K |
| $I$ | current, A |
| $G$ | area to length ratio, cm |
| $N$ | number of pairs of thermoelectric elements |
| $\Delta T_{max}$ | maximum TEC temperature difference at $Q_c$=0, K |
| $I_{max}$ | TEC current at $\Delta T$=$\Delta T_{max}$, A |
| $V_{max}$ | TEC voltage at $\Delta T$=$\Delta T_{max}$, V |
| $Q_{max}$ | maximum $Q_c$ when $\Delta T$=0, W |
| $S_M$ | TEC effective Seebeck coefficient, V/K |
| $R_M$ | TEC effective electrical resistance, Ω |
| $K_M$ | TEC effective thermal conductance, W/K |
| $s$ | Seebeck coefficient, V/K |
| $k$ | thermal conductivity, W/ (cm·K) |

### Greek symbols

| | |
|---|---|
| $\rho$ | electrical resistivity, Ω·cm |

## INTRODUCTION

Electronic components that are utilized in many military applications are required to operate in harsh environments and conditions. A ruggedized electronic component is able to perform in these harsh conditions without decreased performance; however, ruggedizing an electronic component requires increased manufacturing time and cost. Even with continuous improvements in electronic device manufacturing methods, the time required to ruggedize an electronic device is most often equal to or greater than the time required for performance improvement. As a result, the military is often forced to utilize old generation, ruggedized electronic components. Many benefits, such as improved performance, could be realized if state-of-the-art commercial-off-the-shelf (COTS) electronic components were used, especially as add-ons or upgrades to existing devices. However, high-power COTS components may require significant additional cooling in order to maintain lower operating temperatures. Furthermore, the existing cooling system may not be able to support this additional cooling without substantial system redesign, which would result in added time, cost and weight.

Thermoelectrics are solid-state devices capable of converting electrical power directly into cooling while maintaining a temperature differential between the hot and cold sides of the device. Benefits from thermoelectric cooling are best realized when volume reduction, mass reduction, and long term reliability are sought. Furthermore, as a solid-state technology, no moving parts and no working fluids exist, which translates into simple integration, little maintenance, silent operation, and excellent reliability [1]. For relatively simple, steady-state applications, thermoelectric modules are very reliable. In fact, Mean Time Between Failures (MTBFs) in excess of 200,000 hours are not uncommon in such cases and this MTBF value generally is considered to be an industry standard [2].

Thermoelectrics make use of the Peltier effect, which is based on Peltier's observation that passing current through a junction of two dissimilar electrically conductive materials can create cooling (or heating) at the junction. By using doped semiconductors (typically bismuth telluride), the Peltier effect can be exploited to create a thermoelectric heat pump. A typical thermoelectric cooler (TEC) module consists of multiple p-type and n-type elements soldered electrically in series (thermally in parallel) between two ceramic (dielectric) plates. An external electric potential drives the charge carriers in the materials (electrons in n-type, holes in p-type), which also carry thermal energy. The dissimilarities between the properties of the materials at the junctions causes heat to be either rejected or absorbed. A schematic of a single TE cooling element is shown in Figure 1.

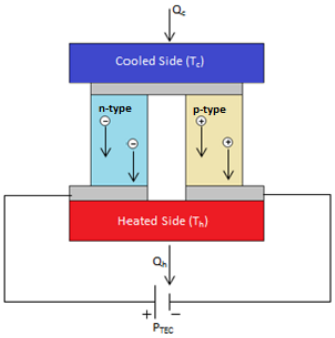


**Figure 1:** A thermoelectric element configured for cooling. A commercial thermoelectric cooler is composed of an array of these elements placed electrically in series and thermally in parallel.

Various TE materials can be compared on an efficiency basis using the figure of merit, *Z,* as calculated in Equation 1.

$$Z = \frac{s^2}{\rho k} \quad (1)$$

The figure of merit represents the relationship between thermal conductivity $k$, electrical resistivity, $\rho$, and Seebeck coefficient $s$ of the thermoelectric material. The operating temperature is the most significant factor when choosing a TE material, as is shown in Figure 2. For relatively low temperature applications, bismuth telluride ($Bi_2Te_3$) demonstrates the highest figure of merit. Alumina is the common choice for the ceramic substrate as it is relatively inexpensive; however, when compared to materials such as aluminum nitride or beryllium oxide, the thermal conductivity of alumina (24 W/m-K) is approximately an order of magnitude less.

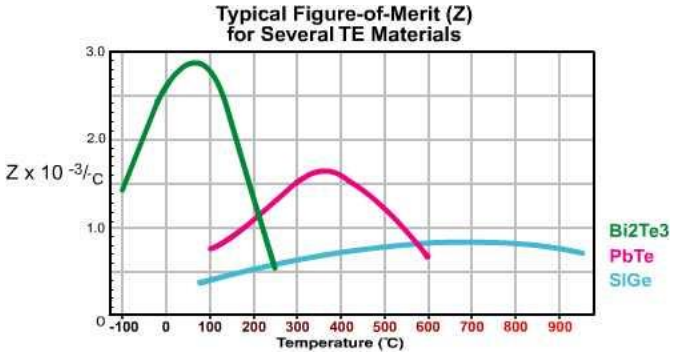


**Figure 2:** Figure of merit, Z, for common TE materials [2].

In order to dissipate the heat from the hot side of a TEC, the TEC must be used in conjunction with a heat exchanger. Depending upon the application, an epoxy or grease thermal interface can be used or the ceramic plates can be metalized and soldered directly to the heat source and heat sink. Thermal stresses, however, must be considered when soldering, and often, soldering isn't viable for applications with significant thermal cycling. As with any thermal management system, minimizing thermal interface resistances is critical to minimizing the overall resistance. Thus, the integration of the TEC is just as important as the selection of the TEC itself.

The theory of thermoelectric phenomena is well understood in the literature [1-4]. Additionally, a number of groups have developed performance models for thermoelectric devices [5-10]. Still, very few resources exist which provide a method for end users to determine the appropriate TEC for their application. Thermoelectric properties are often unclear from manufacturer specifications and performance curves. Furthermore, the role of the thermal interface can be complicated [11]. As a result, it can be difficult to determine how well a TEC will perform in a given scenario. Accordingly, the authors have developed a 1-D thermal model, which predicts the applicability of specific TECs under specific conditions. The authors have also experimentally validated the model via a spot cooling study. Overall, the goal of the study was to demonstrate the viability of utilizing TECs to cool COTS components, under conditions found in military applications, without significant alteration to an existing cooling system.

## THERMAL MODEL DEVELOPMENT

Reduction in component temperatures via TECs may enable the use of COTS components, originally developed for civilian applications, in more demanding military environments. A thermal model was developed to analyze and predict the performance gains that can be achieved by using TECs to assist in the cooling of critical components for avionics applications, where the use of COTS components is highly desirable. The use of TECs in two scenarios was investigated. The first scenario is the use of a TEC for component cooling utilizing a single heat sink on the TEC hot side. The second scenario is the use of a TEC for component cooling utilizing a heat sink on both the component and TEC hot side. The model was developed to simulate both physical configurations and to determine the optimum operating conditions. The model validity was verified by building a test apparatus capable of simulating the two scenarios and allowing for a comparison between the model predictions and experimental measurements.

### Device Level Properties

Thermoelectric material properties such as Seebeck coefficient $s$, electrical resistivity $\rho$, and thermal conductivity $k$, as well as device geometry parameters such as area-to-length ratio $G$, and number of elements $N$, are generally not reported or provided by thermoelectric device manufacturers. Instead, the parameters $V_{max}$, $I_{max}$, $Q_{max}$, and $\Delta T_{max}$ are provided. $V_{max}$ and $I_{max}$ are the voltage and current that occur at $\Delta T_{max}$, the maximum possible temperature difference across the TEC. $\Delta T_{max}$ occurs when the heat absorbed at the cold surface, $Q_c$, is zero. $Q_{max}$ is the maximum amount of heat that can be absorbed at the cold face of the module and occurs at $I_{max}$ when $\Delta T$=0. While these parameters do provide information about the performance of the TEC, they are not easily translated to the physical characteristics needed for design calculations. Instead, Luo has described two separate methods for calculating effective device-level thermoelectric properties that can be useful for module selection and application design [12]. The Figure of Merit for the module can be calculated for hot side temperature $T_h$ (Equation 2) [12].

$$Z = \frac{2\Delta T_{max}}{(T_h - \Delta T_{max})^2} \quad (2)$$

The module effective Seebeck coefficient $S_M$, thermal conductance $K_M$, and electrical resistance $R_M$, can be calculated either from Equations 3-5 or Equations 6-8 [10, 12].

$$S_M = {V_{max}}/{T_h} \quad (3)$$

$$K_M = \frac{(T_h - \Delta T_{max}) V_{max} I_{max}}{2 T_h \Delta T_{max}} \quad (4)$$

$$R_M = \frac{(T_h - \Delta T_{max}) V_{max}}{T_h I_{max}} \quad (5)$$

Or

$$S_M = 2 \frac{Q_{max}}{I_{max}} \frac{1}{T_h + \Delta T_{max}} \quad (6)$$

$$K_M = \frac{T_h - \Delta T_{max}}{T_h + \Delta T_{max}} \frac{Q_{max}}{\Delta T_{max}} \quad (7)$$

$$R_M = \frac{S_M^2}{K_M Z} \quad (8)$$

As noted by Luo, ideally, the effective module properties calculated from the two different methods would match, but in practice they often do not. For the study herein, the difference between the two calculations was approximately 3%. For the thermal model developed in this paper, the average of the two calculated values was used.

The thermoelectric material properties are temperature dependent, and as a result, the effective module properties are as well [3]. The effective module properties can easily vary by 3-10% over the range of hot side temperatures that occur during operation, and manufacturers only provide parameters at two specified hot side temperatures (i.e. $T_h$ = 27°C and 50°C). To increase accuracy in this study, the module properties were linearly interpolated between the values at these hot side temperatures and incorporated in the thermal model. This thermal model has been used to investigate use of TECs in two scenarios.

### Single Heat Sink

In this study, a 1-D thermal resistance network was developed to simulate the performance of a COTS component cooled via a TEC with a single heat sink (Figure 3) [13]. The component was assumed to be thermally insulated on one side and cooled by a TEC on the other.

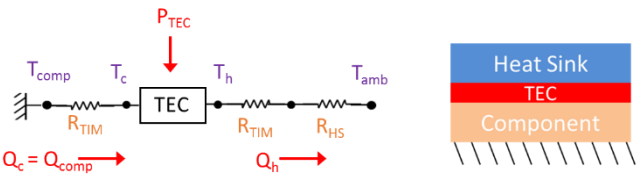


**Figure 3:** Single heat sink thermal resistance model.

The heat flow across a thermoelectric element can be described through equations found in the literature [2-4]. The heat absorbed at the cold face of the TEC, $Q_c$, and the heat rejected at the hot face, $Q_h$, are given by Equations 9 and 10.

$$Q_c = S_M I T_c - \frac{1}{2} I^2 R_M - K_M (T_h - T_c) \quad (9)$$

$$Q_h = S_M I T_c + \frac{1}{2} I^2 R_M - K_M (T_h - T_c) \quad (10)$$

Applying the conservation of energy yields Equation 11, which describes the electrical power generated by the thermoelectric module, $P_{TEC}$.

$$P_{TEC} = Q_h - Q_c = S_M I (T_h - T_c) + I^2 R_M \quad (11)$$

Using these relationships, the thermal resistance network model defines a system of equations that can be analytically solved for the temperatures of interest throughout the system. It is also possible to determine the optimum TEC current, which maximizes performance and minimizes component temperature.

### Dual Heat Sink

The thermal models for the single heat sink and dual heat sink are very similar (Figure 4). The major difference between the two models is the addition of a second heat transfer path from the component. In the dual heat sink scenario, the component is mounted on a liquid cold plate which handles the majority of the heat load. In addition to reducing the component temperature, the goal of using a thermoelectric cooling solution is to remove a larger portion of the heat load with an additional heat sink. This will allow reduction of the coolant temperatures exiting the cold plate, such that it can effectively cool downstream components.

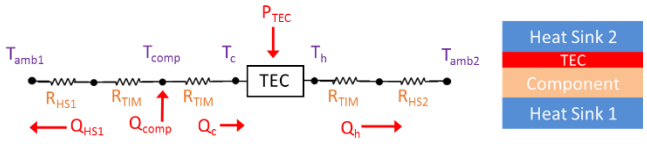


**Figure 4:** Dual heat sink thermal resistance model.

## EXPERIMENTS

### Experimental Setup

An experimental setup was designed and fabricated to validate the results from the thermal model. Tests were conducted at several heat loads with two modules. The two TECs used were TE Technologies Model No. TE-127-1.4-2.5, and Model No. HP-199-1.4-0.8. These thermoelectric modules were chosen to simulate realistic COTS component power dissipation.

A schematic of the experimental setup is given in Figure 5. The component heat load is simulated by a heater block containing two cartridge heaters. High accuracy thermistors were embedded into the heater block to measure an effective component temperature and characterize the heat fluxes. The heat sinks consisted of liquid cold plates. For the single heat sink scenario, the bottom of the heater block is insulated, while in the dual heat sink scenario, an additional cold plate is used. For the test cases that require a larger heat sink thermal resistance, a stainless steel shim is placed in the thermal path. Laird Technologies Tflex HR620 Thermal Gap Filler was used as the thermal interface material (TIM). Baseline tests were

completed in order to characterize the thermal resistance of the TIM. The entire fixture was assembled in a well-insulated box.

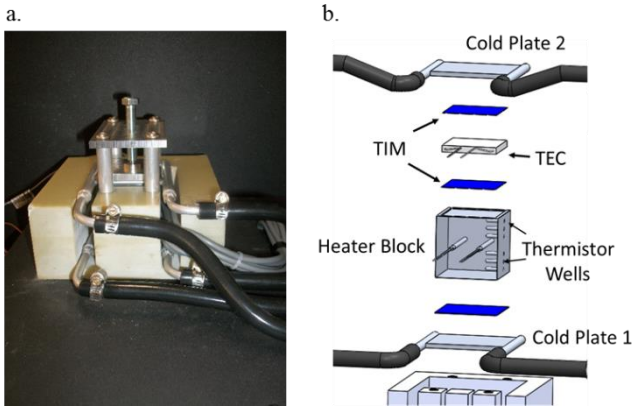


**Figure 5:** a) Thermoelectric test setup b) Schematic of thermoelectric test setup, shown for dual heat sink scenario.

**Single Heat Sink**

In the single heat sink scenario, the baseline consisted of a simulated heat load and a liquid cooled heat sink attached to the heated surface (Figure 6). The heat input was set to 10-30 W (TE-127-1.4-2.5) or 130 W (HP-199-1.4-0.8).


**Figure 6:** Single heat sink scenario with a TEC attached between a cooled component and a heat sink and the baseline case in which the component is attached to a heat sink.

Performance of thermoelectric coolers is dependent on the electrical current applied, and an optimum current can be achieved which minimizes component temperature for a given cooling load. Thus, for testing, current was varied over an appropriate range for each set of tests for comparison to the thermal model. The heat sink thermal resistance was varied to simulate the range of cooling provided by liquid cooling or an air cooled heat sink. The thermal resistance values used during testing are comparable to the air cooling and liquid cooling thermal resistances achieved in avionics applications.

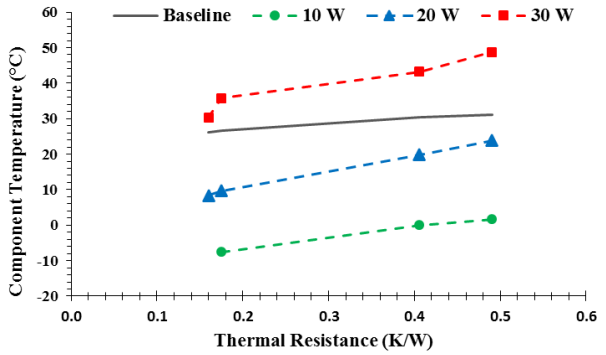


**Figure 7:** Experimental trends for the TE-127-1.4-2.5 TEC at varying component power and system thermal resistance.

Figure 7 provides experimental results for a low power TEC (TE-127-1.4-2.5) and demonstrates that both component power and system thermal resistance will affect the ability of a TEC to cool below baseline conditions. The TEC was operated at 3.5 A, 3.7 A and 3.9 A for the 10 W, 20 W and 30 W case, respectively. At increased thermal resistance and increased power, the low power TEC was not capable of cooling below baseline temperature

Figure 8 shows the results from testing with a low thermal resistance heat sink, which correlates to a COTS component with liquid cooling. These tests were performed with a low power TEC (TE-127-1.4-2.5), at a component power of 30 W. Good agreement between the thermal model and experimental measurements has been achieved. The error between predicted and measured component temperatures did not exceed 3.7 °C, while the predicted optimum current, which minimized component temperature, was within 3.7% of the measured value.

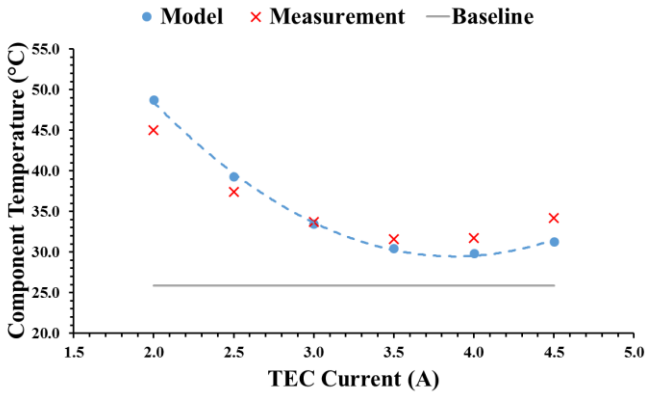


**Figure 8:** Results obtained with a low thermal resistance heat sink and TE-127-1.4-2.5 at a component power of 30 W.

It is worth noting that the component temperature was observed to be higher than the baseline value when utilizing a TEC at high component power (30 W). As is evident from Figure 7, this is partially due to the fact that the thermal interface resistance between the TEC and the component was significantly higher than desired. A thermal gap pad was chosen as the interface material for testing because the configuration needed to be altered many times and thermal grease would have proved troublesome for multiple iterations. The result is a significantly higher interface resistance as compared to typical thermal grease due to the larger thickness and inability to fill all of the surface asperities.

Simulations were performed with the same boundary conditions but with a thermal interface resistance more indicative of thermal grease. Figure 9 shows the results from the simulations illustrating that the thermoelectric cooler provides up to 3°C colder component temperatures as compared to the baseline when a lower interface resistance is applied.

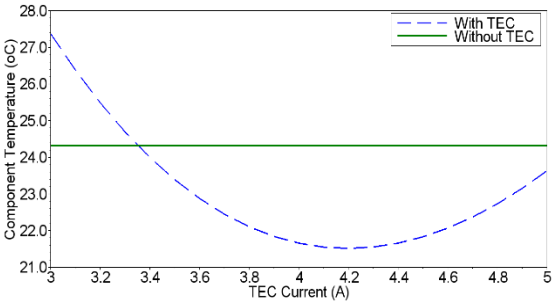


**Figure 9:** Simulated results for a single heat sink at low thermal resistance, when the thermal interface resistance is decreased to 40% of its tested value.

Figure 10 displays the results obtained during testing with the low thermal resistance heat sink and a high power TEC (HP-199-1.4-0.8) with a component power of 130 W. Good agreement between model predictions and component temperatures was observed. The error in measured versus predicted component temperatures did not exceed 3.8 °C over the current range considered. The component temperatures for the higher heat input are significantly higher than the low power case, and the model still accurately predicts the experimental results. This demonstrates the wide range of operating conditions that the model can simulate while still maintaining high fidelity. It is worth noting that higher than baseline component temperature was observed while utilizing a TEC in the higher powered case. Again, this can be attributed to the higher than expected thermal interface resistance.

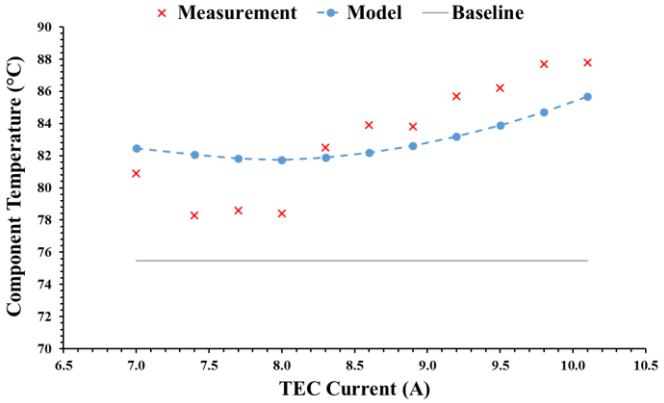


**Figure 10:** Results obtained during testing with a low thermal resistance heat sink with HP-199-1.4-0.8 at a component power of 130 W.

**Dual Heat Sink**

The same experimental setup that was used for the single heat sink case scenario was utilized for the dual heat sink experiments. Figure 11 shows a schematic representation of the baseline and TEC assisted configurations. Experimental results were again used to validate the thermal model.


**Figure 11:** Dual heat sink scenario in which a TEC is placed on one side of a component to increase heat dissipation to one of two heat sinks, and its baseline comparison in which both heat sinks are unassisted.

The heat input (component heat load) was set to either 30 W or 130 W. The same TECs were utilized as in the single heat sink scenario. Electric current was again varied over an appropriate range for each set of tests. The ratio of the thermal resistances of the two heat sinks was also varied to simulate the difference between the liquid cooling of a cold plate and the relatively weak cooling of forced air convection. Three different thermal resistance ratios were investigated during testing. These ratios represent scenarios where the component is liquid cooled and the TEC is air-cooled, the component is air-cooled and TEC liquid cooled, and when both the TEC and component are liquid cooled.

All of the tests conducted showed good agreement between the model's predicted component temperature and the observed component temperature. Error in predicted versus observed component temperatures did not exceed 3.5°C. Figure 12 shows the results for the case where the component is cooled from the bottom by a high thermal resistance and the TEC is cooled with a low thermal resistance. The addition of a TEC resulted in a reduction of the component temperature as compared to the baseline case.

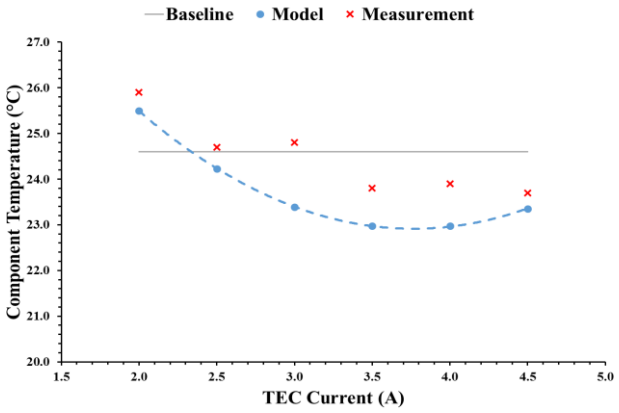


**Figure 12:** Results for the testing case where Heat Sink 1 had a high thermal resistance and Heat Sink 2 had a low thermal resistance at a component power of 30 W.

When the component power is increased to 130 W, the thermoelectric module caused an increase in the component temperature, as seen in Figure 13. The major reason for this result is again attributed to the higher than desired interface resistance between the component and the heat sinks. The effect of higher resistance is amplified at higher powers and provides larger temperature increases.

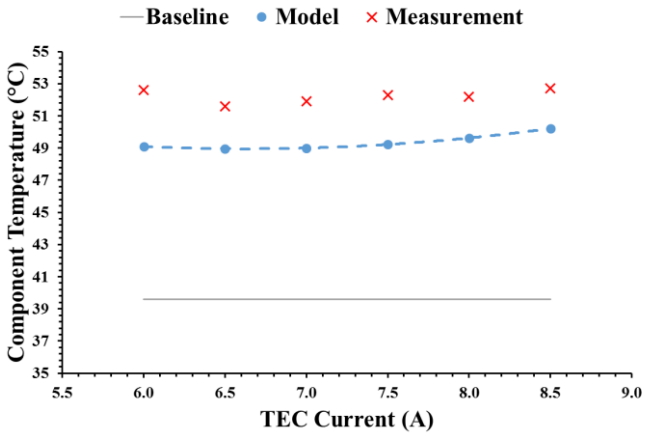


**Figure 13:** Results for the testing case where Heat Sink 1 had a high thermal resistance and Heat Sink 2 had a low thermal resistance at a component power of 130 W.

The thermal model was used to simulate the same case with a 40% lower interface resistance to determine if an improvement in performance could be achieved for this scenario. Figure 14 shows the results from the model indicating that only a marginal reduction in component temperature can be achieved with a TEC in the high power case.

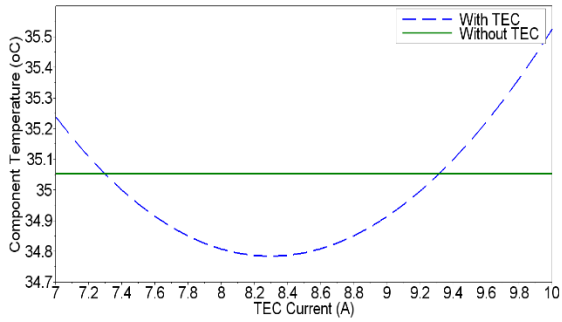


**Figure 14:** Simulations for Figure 13 with a 40% lower thermal interface resistance.

In additional tests, the TEC was able to reduce the component temperature below that which would have been achieved with the heat sink alone, and the model has predicted the measurements very accurately (Figure 15). The error in component temperature predicted versus measured did not exceed 0.4°C. Similar results were achieved in additional tests. These tests provide evidence that the thermal model described in Figure 4 can be used to estimate the performance of designed thermoelectric cooling systems.

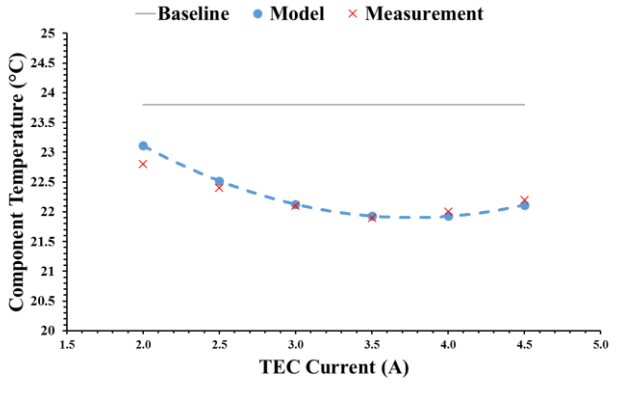


**Figure 15:** Results obtained at 30 W and equal heat sink thermal resistance values.

Figure 16 shows the heat distribution for the previously described test in which the addition of the TEC reduced the cooling load on the lower resistance heat sink by nearly 10%. This provides indication that the addition of a TEC can aid in the distribution of the component heat load. The thermoelectric module permits the transfer of a larger portion of the component heat load to the higher thermal resistance sink. This is beneficial because it can potentially allow the liquid cold plate to operate at a lower temperature, which results in more effective cooling of downstream components.

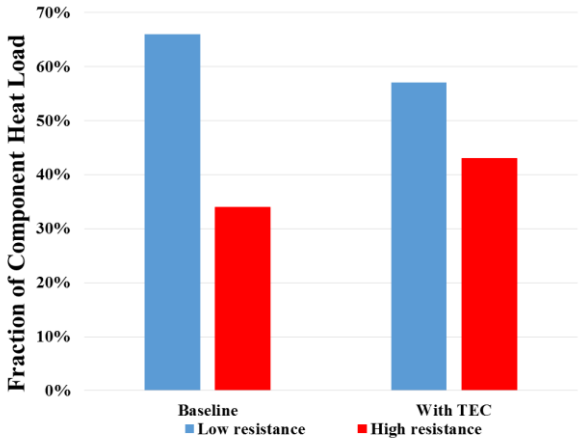


**Figure 16:** Distribution of component heat load dissipation through the two heat sinks (one with high resistance and one with low resistance), with and without the use of TEC.

**Discussion**

The experiments conducted in this study indicate that, under certain conditions, the use of a TEC for component cooling can reduce observed component temperature, especially when an effort is made to minimize the TIM and heat sink thermal resistances. Additionally, experiments with dual heat sinks demonstrated the ability to more evenly distribute component heat load dissipation between the two sinks.

The experimentally measured component temperatures are in general agreement with those predicted by the thermal model, with varying degrees of error. A number of sources can contribute to the difference between the model and experimental values. One significant source of uncertainty is the value of the TIM thermal resistance used in the model.

Baseline measurements indicated that this resistance could vary by up to 50% during an experiment. The reported model results used the mean measured TIM thermal resistance value.

Another source of error may be attributed to averaging of the calculated module properties from the two methods, and the temperature dependence of these properties. Furthermore, number of experimental factors, including the cold plate flow rates and temperatures, the applied clamping force, and the power supplied to the heater block, could result in uncertainty in the measured values.

Finally, it should be noted that the thermal model developed assumes one-dimensional thermal transport in what is a three-dimensional system. Heat spreading and loss into the insulated box will introduce error into the measurement as well.

## DESIGN TOOL DEVELOPMENT

One advantage of the model developed in this study is that one may determine whether thermoelectric cooling is favorable, under certain conditions, for a particular thermoelectric module. This model would be most valuable if it could be generally applied by an end user to determine whether a particular TEC could be applied for their particular scenario. To illustrate this, TEC performance maps have been developed for the single heat sink and dual heat sink models described in the previous sections, which serve as a basis for the development of a TEC Design Tool.

Conceptually, the performance maps are meant to serve a purpose similar to performance maps developed for pumps. Each performance map is valid for particular TEC specifications and scenarios. In Figure 17, a performance map is provided for the single heat sink scenario for a TE-127-1.4-2.5 TEC at optimum current. The curves represent isotherms of the temperature relative to the baseline temperature. If the desired temperature change and actual component heat flux to the TEC are known by the end user, the performance map allows for determination of the required heat sink resistance to achieve the desired temperature change.

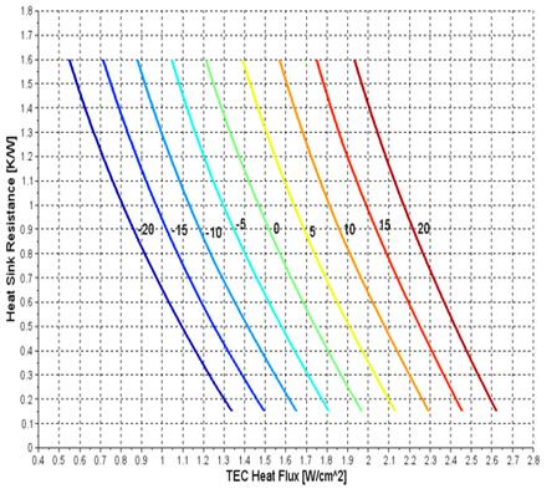


**Figure 17:** Performance map for the TE-127-1.4-2.5 TEC in the single heat sink scenario, which provides anticipated cooling for varying heat sink resistance and heat flux from the component to the TEC.

A similar performance map was developed for the dual heat sink scenario for a TE-127-1.4-2.5 TEC operating at optimum current (Figure 18). In the dual heat sink scenario, isotherms are again determined, but in this case, they are determined for a specified heat flux. Again, if the end user has a desired temperature change and a known component heat flux to the TEC, the performance map verifies scenarios in which the two heat sinks will provide the desired temperature drop.

Performance mapping allows the end user to determine the suitability of a particular module for their scenario and could be useful in the design of future military applications including: electronics cooling, laser diodes, optics, etc. The authors are currently investigating additional thermoelectric modules in order to increase the available database.

Ultimately, the design tool developed from these performance charts should not only indicate when a particular TEC will provide the desired performance, but also indicate what particular TEC is best suited for the scenario. Future work will be focused on enhancing the development tool so that such a determination can be provided to the end user.

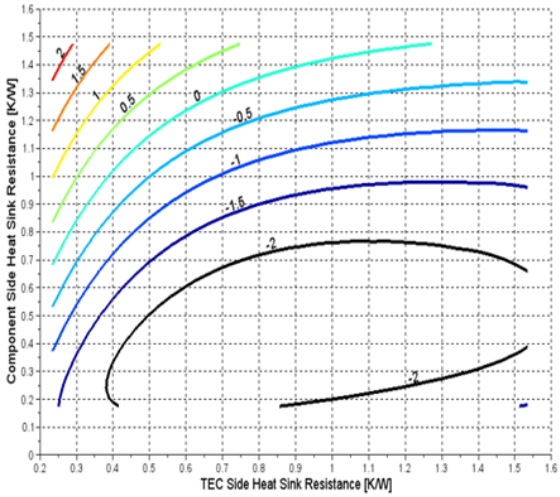


**Figure 18:** Performance map for the TE-127-1.4-2.5 TEC in dual heat sink scenario, which provides anticipated cooling for varying heat sink resistances.

## SUMMARY AND CONCLUSION

The results obtained indicated agreement between the thermal model and experimental results within 3-10% accuracy. The models can be used to quickly investigate the applicability of a TEC to a given scenario and to determine an optimum operating current for a TEC to maximize performance. The models developed can be valuable assets in the development of future prototype TEC systems.

Additionally, the tests conducted indicate that the use of a TEC for component cooling can reduce observed component temperature significantly under certain conditions. However, testing indicates that the use of a TEC can also result in a decrease in performance. Regardless, the model developed is able to predict the outcome. Model predictions indicate that reductions in thermal interface resistance can result in improved performance with the use of TEC under otherwise identical testing conditions.

The work presented here provides the foundation for the development of a design tool that can be used to quickly evaluate the applicability of thermoelectrics for a given electronics cooling application. This design tool would aid in the selection of an appropriate thermoelectric module and in the design of the application. Additional testing needs to be completed in a wider range of operating conditions, as well as with a larger number of thermoelectric modules from different manufacturers, to further validate the model.

## ACKNOWLEDGEMENTS

The work was supported by the Navy Small Business Innovation Research Grant (SBIR), under Contract No. N68335-13-C-0129. Phil Texter was the technician responsible for setting up and conducting the measurements of the thermoelectric cooling modules.

## REFERENCES

[1] L. Bell, "Cooling, Heating, Generating Power, and Recovering Waste Heat with Thermoelectric Systems," Science, vol. 321, no. 5895, pp. 1457-1461, 2008.

[2] Ferrotec Corporation. *Thermoelectric Technical Reference Guide* [online].

[3] CRC Press, *CRC Handbook of Thermoelectrics*, Edited by D. M. Rowe, 1995.

[4] H. J. Goldsmid, *Introduction to Thermoelectricity*, Berlin: Springer, 2010.

[5] K. Fukutani, and A. Shakouri. "Design of Bulk Thermoelectric Modules for Integrated Circuit Thermal Management," IEEE Transactions on Components and Packaging Technologies, vol. 29, no. 4, pp. 750-757, 2006.

[6] P. G. Lau and R. J. Buist, "Temperature and Time Dependent Finite-element Model of a Thermoelectric Couple." 15th International Conference on Thermoelectrics, Pasadena, CA, pp. 227-233, 1996.

[7] W. Seifert et al., "One Dimensional Modeling of a Peltier Element," 20th International Conference on Thermoelectrics, Beijing, China, pp. 439-443, 2001.

[8] G. J. Snyder et al., "Hot Spot Cooling Using Embedded Thermoelectric Coolers," IEEE 22nd Annual Semiconductor Thermal Measurement and Management Symposium, Dallas, TX, pp. 135-143, 2006.

[9] H. Lee, "Optimal Design of Thermoelectric Devices With Dimensional Analysis," Applied Energy, vol. 106, pp. 79-88, 2013.

[10] S. Lineykin and S. Ben-Yaakov, "Modeling and Analysis of Thermoelectric Modules," IEEE Transactions on Industry Applications, vol. 43, no. 2 pp. 505-512, 2007.

[11] B J. Huang, et al., "A Design Method of Thermoelectric Cooler," International Journal of Refrigeration, vol. 23, no. 3, pp. 208-218, 2000.

[12] Luo, Z., "A Simple Method to Estimate the Physical Characteristics of a Thermoelectric Cooler from Vendor Datasheets," Electronics Cooling, vol. 14, no. 3, pp. 22-27, Aug. 2008.

[13] G. L. Solbrekken et al., "Chip Level Refrigeration of Portable Electronic Equipment Using Thermoelectric Devices," International Electronic Packaging Technical Conference and Exhibition, Maui, HI, vol. 2, pp. 647-652, Jul. 2003.